NANOSYSTEMS:
PHYSICS, CHEMISTRY, MATHEMATICS

Rakhmanov S.Z., et al. *Nanosystems: Phys. Chem. Math.*, 2023, **14** (2), 164–171.
http://nanojournal.ifmo.ru
DOI 10.17586/2220-8054-2023-14-2-164-171

Original article

Optical high harmonic generation in a quantum graph

Saparboy Z. Rakhmanov[1,a], Ikhvoliddin B. Tursunov[2,b], Khikmatjon Sh. Matyokubov[3,c], Davron U. Matrasulov[4,d]

[1]Chirchik State Pedagogical University, Chirchik, Uzbekistan

[2] National Universty of Uzbekistan, Vuzgorodok, Tashkent, Uzbekistan

[3] Urgench State University, Urgench, Uzbekistan

[4] Turin Polytechnic University in Tashkent, Tashkent, Uzbekistan

[a]saparboy92@gmail.com, [b]ixvoliddin.tursunov.1998.04.07@gmail.com, [c]hikmat0188@mail.ru, [d]dmatrasulov@gmail.com

Corresponding author: Saparboy Z. Rakhmanov, saparboy92@gmail.com

ABSTRACT High ordered harmonic generation in a quantum graph is studied by considering quantum star graph interacting with external monochromatic optical field. Using the numerically obtained solutions of the time-dependent Schrödinger equation on quantum graph, main characteristics of high harmonic generation are computed. In particular, time-dependence of the average dipole moment and high harmonic generation spectra, determined as the generated field intensity as a function of harmonic order are analyzed. Extension of the proposed model to the case of other graph topologies and application to the problem of tunable high harmonic generation are discussed.

KEYWORDS quantum graphs, optical high harmonic generation, average dipole moment, harmonic generation spectra, quantum graph in electromagnetic field.

ACKNOWLEDGEMENTS This work is supported by the grant of the Ministry of Innovative Development of the Republic of Uzbekistan, World Bank Project “Modernizing Uzbekistan National Innovation System” (Ref. Nr. REP-05032022/235).

FOR CITATION Rakhmanov S.Z., Tursunov I.B., Matyokubov Kh.Sh., Matrasulov D.U. Optical high harmonic generation in a quantum graph. *Nanosystems: Phys. Chem. Math.*, 2023, **14** (2), 164–171.

1. Introduction

Study of the nonlinear optical phenomena occurring in quantum regime is of importance for many practically important tasks appearing in the intersection such topics as quantum optics, atom optics, and optoelectronics. From the viewpoint of fundamental research, the importance of such studies is related to attosecond physics and the physics of ultrafast phenomena, while the practical importance is caused by the relevance to high-power laser generation, optical materials design and optoelectronic device fabrication. An interesting aspect of this topic is optical harmonic generation in quantum regime, which attracted much attention recently [1, 2] in the context of atomic physics and some confined low-dimensional quantum systems, such as quantum wells and dots. One of the main tasks in this field is achieving slowly-decaying (as a function of harmonic order) harmonic generation intensity. Solving of such problem is complicated due to the typical features of the harmonic emission spectra of an atom in a strong optical field, which are known as “the plateau” and “the cutoff”. These latter are a wide frequency region with harmonics of comparable intensities, and an abrupt intensity decrease at the end of the plateau. Physical mechanisms of such effects have been explained within the so-called “three-step” model. Existence of such effect makes difficult generating of very high order harmonics and ultrashort pulses, as their intensity becomes very small at high harmonic orders. Therefore, revealing of the high harmonic generation (HHG) regime, where the intensity would slowly decay as a function of harmonic order is of importance for different practical tasks. Study of HHG in low-dimensional quantum systems can be one of the ways providing achieving of such a goal. In this paper, we address the problem of optical high harmonic generation in branched quantum wires. These latter are modeled in terms of the quantum graphs, which are determined as a set of wires connected to each other according to a rule, called topology of the graph [3–5]. Generation of the topical harmonics is assumed as to be caused by the interaction of branched quantum wires with an external monochromatic optical field. Using the eigenfunctions of the quantum graph, we compute numerically the average dipole moment as a function of generated frequencies. Also, as the main characteristics of the high harmonic generation process, we compute the spectrum of the high harmonic generation which is determined as the intensity of the field generated by the interaction of the branched quantum wire with the external optical field. Earlier, quantum graphs have attracted much attention in different contexts for modeling particle and quasiparticle dynamics in branched structures (see Refs. [3–16]).

2. Schrödinger equation on graphs

Here we briefly recall basic quantum graphs theory following Refs. [4, 10]. Graphs are the systems consisting of vertices which are connected by edges. The edges are connected according to a rule which is called the topology of the graph. Topology of the graph is described in terms of the adjacency matrix [4, 5]:

$$C_{ij} = C_{ji} = \begin{cases} 1, & \text{if } i \text{ and } j \text{ are connected;} \\ 0, & \text{otherwise;} \end{cases} \qquad i, j = 1, 2, ..., N.$$

Earlier, quantum graphs were extensively studied in the context of quantum chaos theory [4–6]. Strict mathematical formulation of the boundary conditions was given by Kostrykin and Schrader [3]. Inverse problems on quantum graphs have been studied in Refs. [7–9]. An experimental implementation of quantum graphs on (optical) microwave waveguide networks is discussed in the Ref. [8]. Despite the fact that different issues of quantum graphs and their applications have been discussed in the literature, the problem of driven graphs is still remaining as less-studied topic.

Quantum particle dynamics on a graph is described by one-dimensional multi-component Schrödinger equation [4,5] (in the units $\hbar = 2m = 1$):

$$-\frac{d^2\phi_b(x)}{dx^2} = k^2\phi_b(x), \quad b = (i, j), \tag{1}$$

where b denotes a bond connecting i-th and j-th vertices, and for each bond b, the component ϕ_b of the total wave function ϕ is a solution of Eq. (1). In Eq. (1) components are related through the boundary conditions, providing continuity and current conservation [4]:

$$\begin{cases} \bullet \text{ Continuity,} \\ \phi_{i,j}|_{x=0} = \varphi_i, \;\; \phi_{i,j}|_{x=L_{i,j}} = \varphi_j \;\; \text{for all} \;\; i < j \;\; \text{and} \;\; C_{i,j} \neq 0. \\ \bullet \text{ Current conservation,} \\ -\sum\limits_{j<i} C_{i,j} \dfrac{d\phi_{j,i}(x)}{dx}\Big|_{x=L_{i,j}} + \sum\limits_{j>i} C_{i,j} \dfrac{d\phi_{i,j}(x)}{dx}\Big|_{x=0} = \lambda_i\varphi_i. \end{cases} \tag{2}$$

Here, the parameters λ_i are free parameters which determine the type of boundary conditions. The Dirichlet boundary conditions correspond to the case when all the $\lambda_i = \infty$. Solution of Eq. (1) obeying the above boundary conditions can be written as

$$\phi_{i,j} = \frac{C_{i,j}}{\sin kL_{i,j}}(\varphi_i \sin k(L_{i,j} - x) + \varphi_j \sin kx),$$

where the quantities φ_i are the solutions of the algebraic system following from the continuity conditions:

$$\sum_{j\neq i} \frac{kC_{i,j}}{\sin kL_{i,j}}(-\varphi_i \cos kL_{i,j} + \varphi_j) = \lambda_i\varphi_i.$$

The eigenvalues of Eq. (1) can be found from the spectral equation

$$\det\left(h_{i,j}(k)\right) = 0 \tag{3}$$

where

$$h_{i,j}(k) = \begin{cases} -\sum\limits_{m\neq i} C_{i,m} \cot kL_{i,m} - \dfrac{\lambda_i}{k}, & i = j \\ C_{i,j} \sin^{-1} kL_{i,j}, & i \neq j \end{cases}$$

Here we focus on the simplest graph topology, star graph. In this case, since the graph has only single non-boundary vertex, unlike the notations in Eqs. (1) and (2), indices are assigned to the bonds (not to the vertices), i.e. L_j means j-th bond. Thus, in special case of star graph, the boundary conditions can be written as [10]

$$\begin{cases} \phi_1|_{y=0} = \phi_2|_{y=0} = ... = \phi_N|_{y=0}, \\ \phi_1|_{y=L_1} = \phi_2|_{y=L_2} = ... = \phi_N|_{y=L_N} = 0, \\ \sum\limits_{j=1}^{N} \dfrac{\partial}{\partial y}\phi_j|_{y=0} = 0. \end{cases} \tag{4}$$

The eigenvalues of star graph can be found from the following spectral equation [10]

$$\sum_{j=1}^{N} \tan^{-1}(k_n L_j) = 0. \tag{5}$$

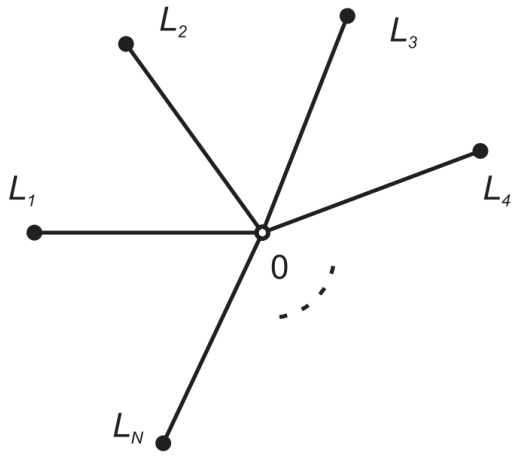

FIG. 1. Sketch of a metric star graph. L_j is the length of the j th bond with j=1, 2,. ..,N

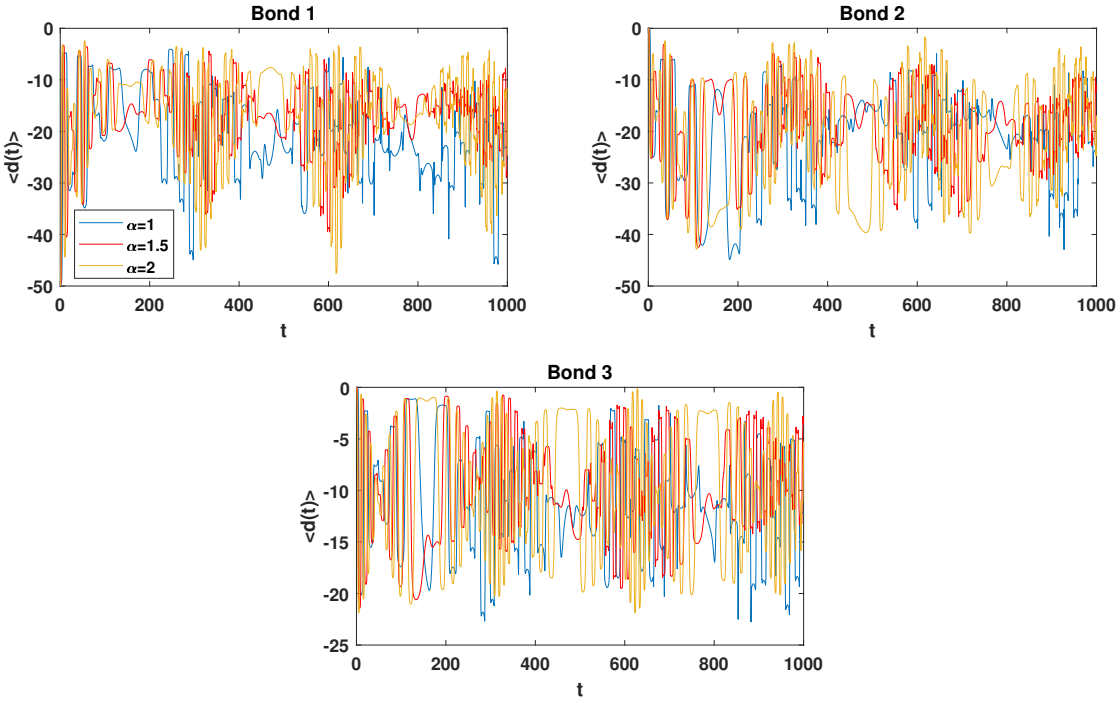

FIG. 2. Average dipole moment as a function of time on star graph at different values of α parameter for external field's amplitude, $\epsilon = 0.1$ and frequency, $\omega_0 = 0.01$

Corresponding eigenfunctions are given as [10]

$$\phi_{j,n} = \frac{B_n}{\sin(k_n L_j)} \sin(k_n(L_j - y)), \tag{6}$$

where

$$B_n = \sqrt{\frac{2}{\sum_j \frac{L_j + \sin(2k_n L_j)}{\sin^2(k_n L_j)}}}.$$

The functions $\phi_{j,n}$ are orthonormal, i.e., fulfill the following condition:

$$\sum_{j=1}^{N} \int_0^{L_j} \phi^*_{j,m}(x)\phi_{j,n}(x)dx = \delta_{mn}. \tag{7}$$

In the next section, we use these eigenfunctions for computing the high harmonic generation spectrum.

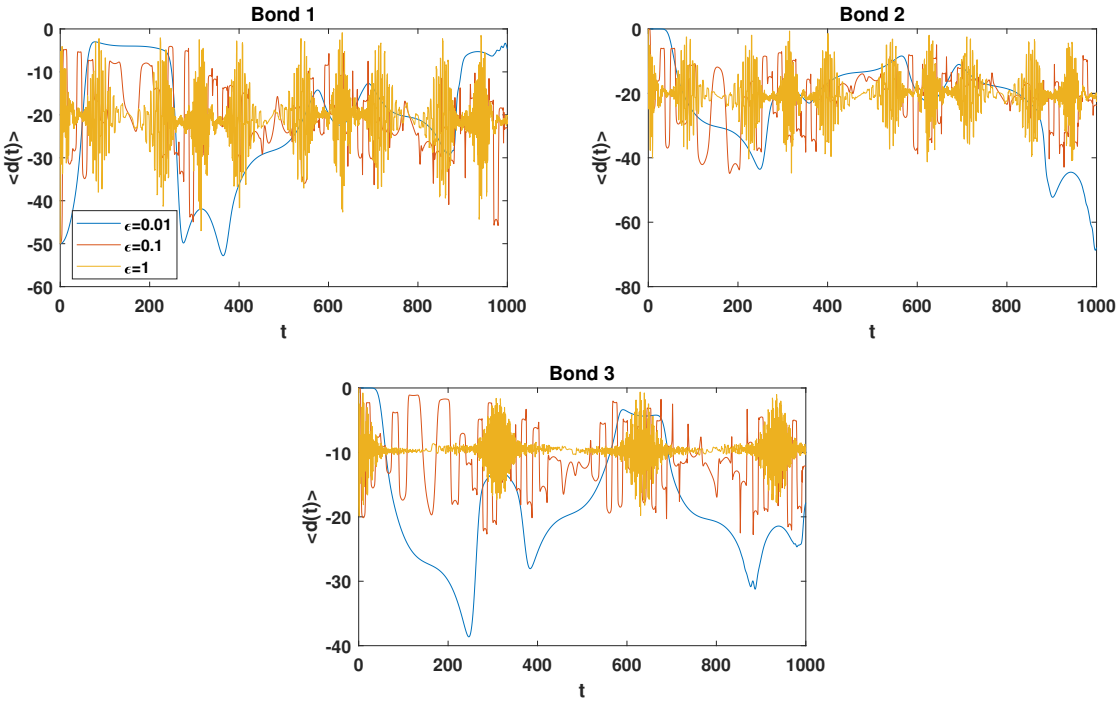

FIG. 3. Average dipole moment as a function of time on star graph at different values of amplitude of the external field for field's frequency, $\omega_0 = 0.01$, for length of each bond, $L_1 = 200.31$, $L_2 = 205.53$ and $L_3 = 210.18$

3. Driven star graph by external potential

Consider a quantum star graph (Y-junction) interacting with an external linearly polarized monochromatic electromagnetic field. Such system can be described by the following time-dependent (multi-component) Schrödinger equation:

$$i\frac{\partial \Psi_j(x,t)}{\partial t} = \left[-\frac{d^2}{dx^2} + \epsilon x \cos\omega_0 t\right]\Psi_j(x,t), \qquad j = 1,2,3, \tag{8}$$

where ϵ and ω_0 are the amplitude and the frequency of the optical field, respectively.

The solution of Eq. (8) can be written in terms of the complete set of solutions of Eq. (1)

$$\Psi_j(x,t) = \sum_n C_n(t)\phi_{j,n}(x), \tag{9}$$

where $\phi_{j,n}(x)$ are given by Eq. (6).

Substituting (9) into Eq. (8) and using the condition given by Eq. (7), we get a system of first order ordinary differential equations which has the form

$$i\dot{C}_n(t) = \varepsilon_n C_n(t) + \sum_m C_m(t)V_{nm}, \tag{10}$$

where

$$V_{nm} = \sum_j \int_0^{l_j} \phi^*_{j,n}\hat{V}(t)\phi_{j,m}dx = \epsilon\cos\omega_0 t \sum_j \int_0^{l_j} x\phi^*_{j,n}\phi_{j,m}dx$$

and ε_n are the eigenvalues of the unperturbed system.

Using numerically found solutions of Eq. (8), one can compute physically observable characteristics of the system "quantum star graph + external optical field".

In numerical calculations, we choose the Gaussian wave packet given on the first bond of the graph as the initial state:

$$\Psi_1(x,0) = \Phi(x) = \frac{1}{\sqrt{2\pi}\sigma}e^{-\frac{(x-\mu)^2}{2\sigma}}, \tag{11}$$

with σ being the width of the packet. For other bonds, the initial wave function is assumed to be zero, i.e. $\Psi_2(x,0) = \Psi_3(x,0) = 0$.

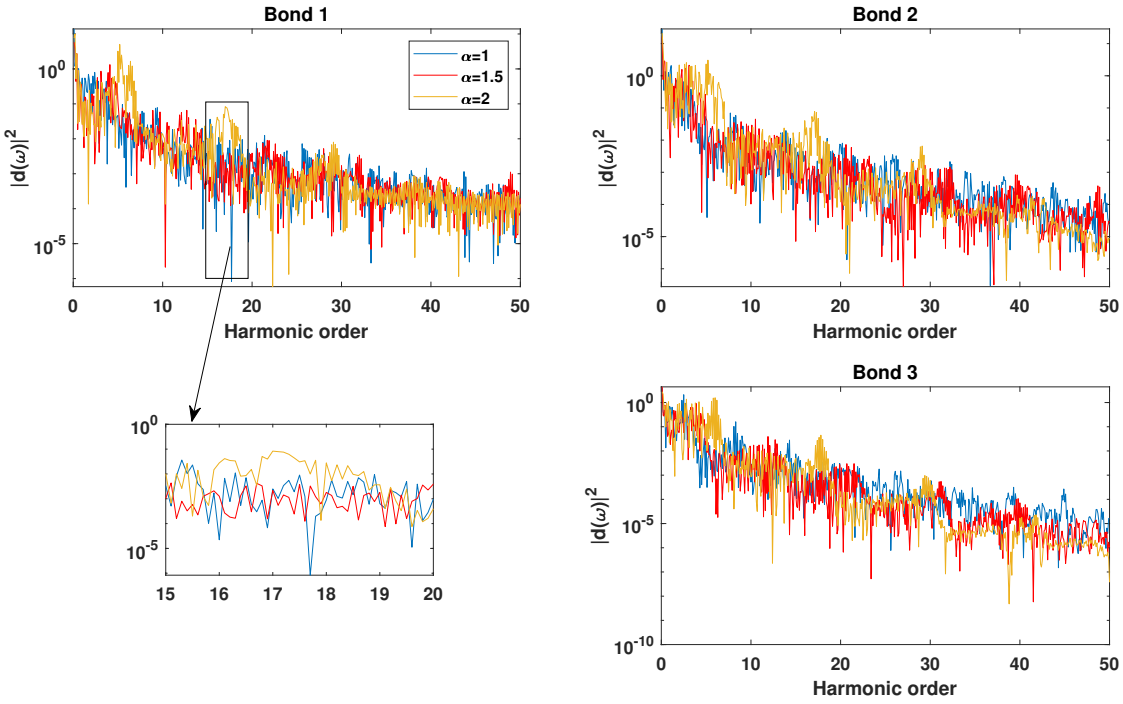

FIG. 4. Spectrum of harmonic generation on star graph at different values of α parameter for external field's amplitude, $\epsilon = 0.1$, and frequency, $\omega_0 = 0.01$, for duration of interaction, $T = 1000$

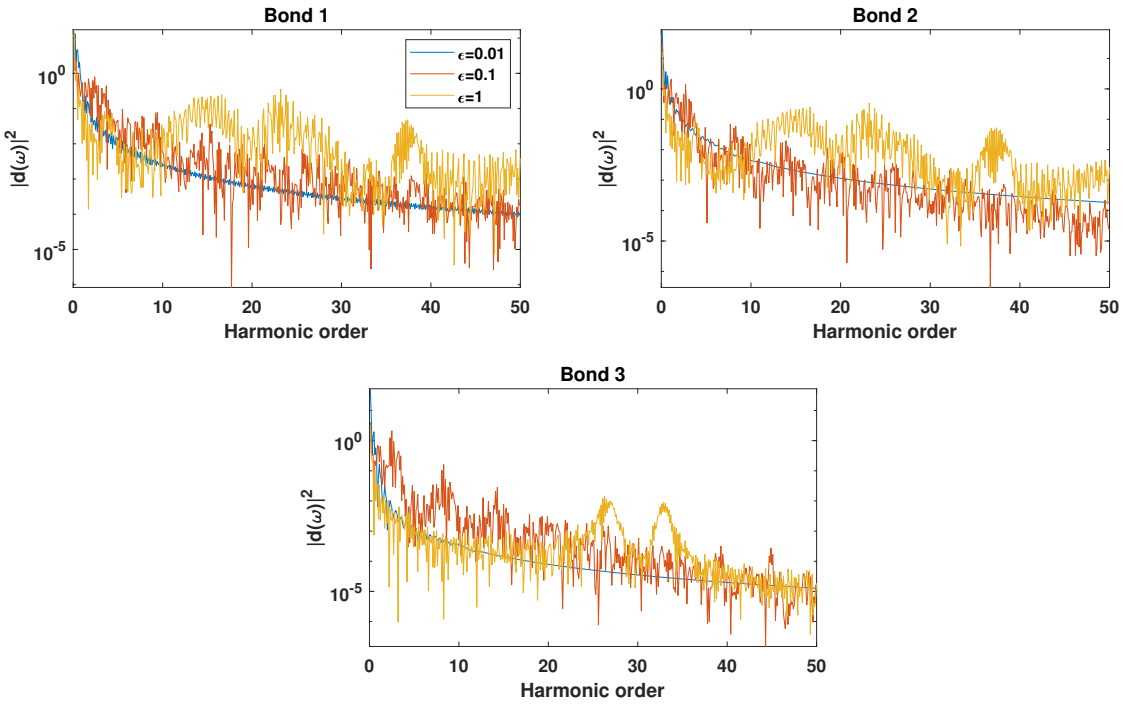

FIG. 5. Spectrum of harmonic generation on star graph at different values of amplitude of external field for field's frequency, $\omega_0 = 0.01$, for length of each bond, $L_1 = 200.31$, $L_2 = 205.53$ and $L_3 = 210.18$, for duration of interaction, $T = 1000$

For such initial conditions, the expansion coefficients at $t = 0$ can be written as

$$C_n(0) = \int_0^{l_1} \Phi(x)\phi_{1n}^*(x)dx.$$

4. High harmonic generation in star graph

Consider high harmonic generation caused by the interaction of the quantum star graph with the external monochromatic optical field. One of the main characteristics of such process is the average (expectation) value of the dipole moment which is determined as [1]

$$\langle d_j(t)\rangle = -\langle \Psi_j(x,t)|x|\Psi_j(x,t)\rangle, \qquad j = 1,2,3.$$

To compute $\langle d_j(t)\rangle$, one can use the solution of Eq. (8). In terms of the expansion coefficients in Eq. (9), one can write the average dipole moment as

$$\langle d_j(t)\rangle = -\sum_{m,n} C_m^*(t)C_n(t)\tilde{V}_{jmn},$$

where $\tilde{V}_{jmn} = \int_0^{L_j} x\phi_{j,n}^*\phi_{j,m}dx$.

In the following, all the plots are produced by choosing the initial state as Gaussian wave packet determined in Eq. (11) and coming from the first bond. Furthermore, we choose the bond lengths as $L_j = \alpha l_j$. The width and the initial position of the packet are fixed as $\sigma = 10$, $\mu = 50$, respectively. Fig. 2 presents the plots of the average dipole moment for star graph with the bond lengths, $l_1 = 200.31$, $l_2 = 205.53$ and $l_3 = 210.18$, as a function of time at different values of α. The amplitude and the frequency of the electromagnetic field are taken as $\epsilon = 0.1$ and $\omega_0 = 0.01$, respectively. As it can be seen from this plot, $\langle d_j(t)\rangle$ is quasi periodic in time and the period decreases as the parameter α increases.

In Fig. 3, plots show time-dependence of the average dipole moment of each bond at different values of amplitude of the external field strength, $\epsilon = 0.01$ (blue line), $\epsilon = 0.1$ (red line) and $\epsilon = 1$ (yellow line). One can see the strong dependence on the amplitude of the electromagnetic field. Period of the quasi periodic average dipole moment decreases as the amplitude of the electromagnetic field grows.

Another important characteristics of the high harmonic generation in quantum regime is its spectrum which is determined in terms of its intensity on each bond (as a function of frequency generated) and given as

$$I_j(\omega) = |d_j(\omega)|^2 = \left| \frac{1}{T}\int_0^T e^{-i\omega t}\langle d_j(t)\rangle dt \right|^2, \tag{12}$$

where T is the total duration of interaction of the quantum graph with the external optical field. The total harmonic generation intensity is defined as the sum of those on each bond. The main practically relevant feature of the high harmonic generation intensity is the appearance of "the plateaus" at certain values of the generated frequency. In other words, the high harmonic generation spectrum, which is determined as the ratio of the external field frequency and the frquency of generated one, $N = \omega/\omega_0$, consists of a plateau where the harmonic intensity is nearly constant over many orders and a sharp cutoff. As higher the number of plateaus, as attractive the harmonic generation from the viewpoint of attosecond physics and high power laser generation [17,18]. Fig. 4 presents the plot of $I(N)$ on each bond of the quantum star graph for different values of α choosing the field parameters as $\epsilon = 0.1$, $\omega_0 = 0.01$ and $T = 1000$. In Fig. 4, one can see the decreasing of the spectrum as harmonic order increases. Moreover, for large values of the length of bonds, the intensity of high order harmonics increases. Existence of "quasi-plateau" can be seen from the inset. Fig. 5 shows plots of the spectrum of the harmonic generation at different values of the external field strength and field's frequency, $\omega_0 = 0.01$ for bond length chosen as $L_1 = 200.31$, $L_2 = 205.53$ and $L_3 = 210.18$ for duration of interaction, $T = 1000$. The plot shows that the HHG intensity is strongly depends on the field strength. For higher values of ϵ, one can observe increasing of the intensity. The above study can be directly extended to any branching topology of a quantum graph (e.g., tree, hexagon, loop, H-graph, etc). Of course, complicated branching topologies should provide wider opportunity for the HHG-process.

5. Conclusion

In this paper, we studied high harmonic generation in quantum star graph caused by its interaction with the external monochromatic optical field. The average dipole moment as a function of time is analyzed as one of the characteristics of HHG. The harmonic generation spectrum described in terms of the generation intensity as a function of the harmonic order given by the ratio of the generated harmonics to that of the external field, is computed at different values of the external field strength, as well as for different bond lengths. Appearance of narrow plateau was shown by analyzing the plots of the HHG spectra. The model considered in this study can be implemented, e.g., in different quantum wire networks fabricated on the basis of superconductors, semiconductors or other low-dimensional quantum materials. Some versions of such quantum wire networks have been studied earlier in Refs. [19–22]. Extension of the above model to the case of other branching topologies and external (e.g., bi-, or poly-chromatic, or nonlinearly polarized) fields can provide an effective tool for tunable high harmonic generation in low-dimensional structures. In addition, the model can be considered as a version of the quantum graph based laser concept. Such concepts have been earlier discussed in [23–43].

References

[1] Boyd R.W. *Nonlinear Optics*, 2007, 3rd ed, Academic Press.

[2] Tong X., Chu Sh. Theoretical study of multiple high-order harmonic generation by intense ultrashort pulsed laser fields: A new generalized pseudospectral time-dependent method. *Chem. Phys. B*, 1997, **217**(2-3), P. 119–130.

[3] Kostrykin R., Schrader R. Kirchhoff's rule for quantum wires. *J. Phys. A: Math. Gen*, 1999, **32**, P. 595–630.

[4] Kottos T., Smilansky U. Periodic Orbit Theory and Spectral Statistics for Quantum Graphs. *Ann. Phys.*, 1999, **274**, P. 76–124.

[5] Gnutzmann S. and Smilansky U. Quantum graphs: Applications to quantum chaos and universal spectral statistics. *Adv. Phys.*, 2006, **55**, P. 527–625.

[6] Gnutzmann S., Keating J.P., Piotet F. Eigenfunction statistics on quantum graphs. *Ann. Phys.*, 2010, **325**, P. 2595–2640.

[7] Boman J., Kurasov P. Symmetries of quantum graphs and the inverse scattering problem. *Adv. Appl. Math.*, 2005, **35**, P. 58–70.

[8] Hul O., Bauch S., Pakoński P., Savytskyy N., Życzkowski K. and Sirko L. Experimental simulation of quantum graphs by microwave networks. *Phys. Rev. E.*, 2004, **69**, P. 056205/1-7.

[9] Cheon T., Exner P., Turek O. Approximation of a general singular vertex coupling in quantum graphs. *Ann.Phys.*, 2010, **325**, P. 548–578.

[10] Keating J.P. Fluctuation statistics for quantum star graphs. Quantum graphs and their applications. *Contemp. Math.*, 2006, **415**., P. 191–200.

[11] Matrasulov D.U., Yusupov J.R., Sabirov K.K., Sobirov Z.A. Time-dependent Quantum Graph. *Nanosystems: Physics, Chemistry, Mathematics*, 2015, **6**(2), P. 173–181.

[12] Yusupov J.R., Sabirov K.K., Ehrhardt M., Matrasulov D.U. Transparent quantum graphs. *Phys. Lett. A.*, 2019, **383**, P. 2382–2388.

[13] Matrasulov D.U., Sabirov K.K. and Yusupov J.R. PT-symmetric quantum graphs. *J. Phys. A.*, 2019, **52**, P. 155302/1-11.

[14] Nikiforov D.S., Blinova I.V. and Popov I.Y. Schrödinger and Dirac dynamics on time-dependent quantum graph. *Indian J. Phys.*, 2019, **93**(7), P. 913–920.

[15] Yusupov J.R., Sabirov K.K., Asadov Q.U., Ehrhardt M. and Matrasulov D.U. Dirac particles in transparent quantum graphs: Tunable transport of relativistic quasiparticles in branched structures. *Phys. Rev. E.*, 2020, **101**, P. 062208/1-8.

[16] Yusupov J.R., Sabirov K.K. and Matrasulov D.U. Dirac particles on periodic quantum graphs. *Phys. Rev. E.*, 2021, **104**, P. 014219/1-7.

[17] Strelkov V.V., Platonenko V.T., Sterzhantov A.F. and Ryabikin M.Yu. Attosecond electromagnetic pulses: generation, measurement, and application. Generation of high-order harmonics of an intense laser field for attosecond pulse production. *Phys. Uspekhi*, 2016, **59**(5), P. 425–445.

[18] Winterfeldt C., Spielmann C., Gerber G. Optimal control of high-harmonic generation. *Rev. Mod. Phys.*, 2008, **80**(2), P. 117–140.

[19] Kohmoto M. Quantum wire networks with quantized Hall effect. *J. Phys. Soc. Jpn.*, 1999, **62**, P. 4001–4008.

[20] Aharony A., Entin-Wohlman O. Discrete versus Continuous Wires on Quantum Networks. *J. Phys. Chem. B*, 2009, **113**, P. 3676–3680.

[21] Medina J., Green D., Chamon C. Networks of quantum wire junctions: A system with quantized integer Hall resistance without vanishing longitudinal resistivity *Phys. Rev. A., B*, 2013, **87**, P. 045128.

[22] Caudrelier V., Mintchev M., Ragoucy E. Quantum wire network with magnetic flux. *Phys. Lett. A.*, 2013, **377**, P. 1788–1793.

[23] Lepri S., Trono C., Giacomelli G. Complex Active Optical Networks as a New Laser Concept. *Phys.Rev.Lett.*, 2017, **118**, P. 123901.

[24] Rotter S. Network lasers. *Nature Photonics*, 2019, **13**, P. 140–145.

[25] Brabec T., Krausz F. Intense few-cycle laser fields: Frontiers of nonlinear optics. *Rev. Mod. Phys.*, 2000, **72**(2), P. 545–591.

[26] Yousef I., et.al. Relativistic high-power laser matter interactions. *Phys. Rep.*, 2006, **427**(2-3), P. 41–155.

[27] Winterfeldt C., Spielmann C., and Gerber G. Colloquium: Optimal control of high-harmonic generation. *Rev. Mod. Phys.*, 2008, **80**(1), P. 117–140.

[28] Krausz F., Ivanov M. Attosecond physics. *Rev. Mod. Phys.*, 2009, **81**, P. 163–234.

[29] Nisoli M., Sansone G. New frontiers in attosecond science Author links open overlay panel. *Prog. Quant. Electr.*, 2009, **33**, P. 17–59.

[30] Kohler M.C., Pfeifer T., Hatsagortsyan K.Z.,Keitel C.H. Frontiers of Atomic High-Harmonic Generation. *Advances In Atomic, Molecular, and Optical Physics*, 2012, **61**, P. 159–208.

[31] Ahn D., Chuang S.L. Optical gain in a strained-layer quantum-well laser. *IEEE J. Quantum Electron*, 1988, **24**, P. 2400–2406.

[32] Rosencher E., Bois Ph. Model system for optical nonlinearities: Asymmetric quantum wells. *Phys. Rev. B.*, 1991, **44**, P. 11315–11327.

[33] Milanovic V., Ikonic Z., Indjin D. Optimization of resonant intersubband nonlinear optical susceptibility in semiconductor quantum wells: The coordinate transform approach. *Phys. Rev. B.*, 1996, **53**, P. 10887–10893.

[34] Xie W., J.Lumin. The nonlinear optical rectification of a confined exciton in a quantum dot. **131**. P. 943–946.

[35] Li B., Guo K-X., Zhang C.-J., Zheng Y.-B. The second-harmonic generation in parabolic quantum dots in the presence of electric and magnetic fields. *Phys. Lett. A*, 2007, **367**, P. 493–497.

[36] Liu J-T., Su F-H., Wang H. Model of the optical Stark effect in semiconductor quantum wells: Evidence for asymmetric dressed exciton bands. *Phys. Rev. B.*, 2009, **80**, P. 113302/1-4.

[37] Shao Sh., Guo K-X., Zhang Z-H., Li N., Peng Ch. Studies on the second-harmonic generations in cubical quantum dots with applied electric field. *Physica B: Physics of Condensed Matter*, 2011, **406**, P. 393–396.

[38] Karimi M.J., Keshavarz A., Second harmonic generation in asymmetric double semi-parabolic quantum wells: Effects of electric and magnetic fields, hydrostatic pressure and temperature. *Physica E*, 2012, **44**, P. 1900–1904.

[39] Zhai W. A study of electric-field-induced second-harmonic generation in asymmetrical Gaussian potential quantum wells. *Physica B*, 2014, **454**, P. 50–55.

[40] Bondarenko V., Zauzny M. Intrinsic optical intersubband bistability in quantum well structures: Role of multiple reflections. *Phys. Rev. B.*, 2015, **91**, P. 035303/1-20.

[41] Kotova L.V., Platonov A.V., Kats V.N. Optical activity of quantum wells. *Phys. Rev. B.*, 2016, **94**, P. 165309/1-5.

[42] Mohammadi S.A., Khordad R., Rezaei G. Optical properties of a semispherical quantum dot placed at the center of a cubic quantum box: Optical rectification, second and third-harmonic generations. *Physica E*, 2016, **76**, P. 203–208.

[43] Rakhmanov S., Matrasulov D., Matveev V.I. Quantum dynamics of a hydrogen-like atom in a time-dependent box: Cooling, compressing and diffusive ionization in non-adiabatic regime. *Eur. Phys. J. D.*, 2018, **72** P. 177/1-8.

Submitted 14 February 2023; revised 28 March 2023; accepted 29 March 2023

Information about the authors:

S. Z. Rakhmanov – Chirchik State Pedagogical University, 104 Amir Temur Str., 111700, Chirchik, Uzbekistan; ORCID 0000-0001-8569-1709; saparboy92@gmail.com

I. B. Tursunov – National Universty of Uzbekistan, Vuzgorodok, 100174, Tashkent, Uzbekistan; ixvoliddin.tursunov.1998.04.07@gmail.com

Kh. Sh. Matyokubov – Urgench State University, 14 H. Olimjon Str., 220100 Urgench, Uzbekistan; ORCID 0000-0002-6642-5488; hikmat0188@mail.ru

D. U. Matrasulov – Turin Polytechnic University in Tashkent, 17 Niyazov Str., 100095, Tashkent, Uzbekistan; ORCID 0000-0001-8957-0058; dmatrasulov@gmail.com

Conflict of interest: the authors declare no conflict of interest.